

Laser Crystal Phosphor Automobile Headlight Integrated with Beam Control and LiDAR

Y.P. Chang^{1,2}, Alan Wang¹, Wood-Hi Cheng², Kenneth Li³

¹Taiwan Color Optics, Inc., Taichung City, Taiwan

²National Chun Hsing University, Taichung City, Taiwan

³Optonomous Technologies Inc., Agoura Hills, CA, USA

Keywords: Intelligent Headlight, Crystal Phosphor, DMD, LiDAR and Laser Phosphor

ABSTRACT

To allow mass adoption of autonomous vehicles, cost and performance become very important factors. This paper describes the development of high performance crystal phosphor with applications to automobile headlights, smart headlights, and LiDAR such that many limitations are eliminated and through integration, which could lower the cost of the system. A patent pending design of a smart headlight integrated with a LiDAR sensor using a single DMD will be described.

1 Introduction

A new scheme of LiDAR-embedded smart laser headlight module (LHM) for autonomous vehicles is proposed and demonstrated using a commercially LiDAR sensor with the wavelength of 905-nm, whereas the LHM was fabricated by a highly reliable glass phosphor material which exhibited excellent thermal stability, as shown in Figure 1 [1].

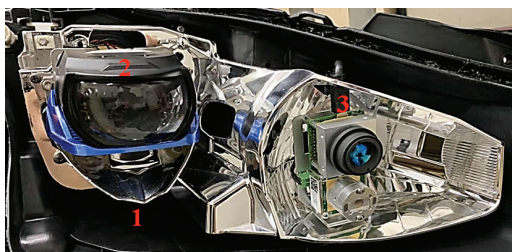


Figure 1 - Integrated smart laser headlight of (1) high-beam LHM, (2) low-beam LEDM, and (3) LiDAR [1].

A new design of an intelligent headlight integrated with a LiDAR sensor using a single DMD is being developed and will be described. Crystal phosphor will be used to further improve the system efficiency and extreme high beam applications.

2 Fabrication of glass phosphor converter layer

The primary benefit for drivers using laser diode (LD) headlights is that the beam usable range can be up to 600-m [2]. This offers the driver improved visibility, contributing significantly to road traffic safety. Most of the white LD engines are integrated using blue LD and phosphor-converter layer. The laser headlights based

phosphor-converted layers had been fabricated using ceramic [3], single crystal [4], and glass materials [5]. However, the fabrication temperatures of the ceramic- and single crystal-based phosphor were over 1200°C and 1500°C, respectively. These high-temperature fabrication requirements had been difficult for the commercial production. In previous reports [6-8], the glass-based phosphor-converter layers made by processes with temperature as low as 750°C had shown to have better thermal stability than that of the silicone-based color conversion layers. The glass-based phosphor with better thermal stability is one of the most promising materials for use in the LD light engines.

The fabrication procedures of glass-based yellow phosphor-converter layer (Ce³⁺: YAG) started with the preparation of sodium mother glass by melting the mixture of the raw materials at 1300°C and dispersing Ce³⁺: YAG powders into the mixture by gas-pressure and sintering under different temperatures [6-8]. The composition of the sodium mother glass was 60 mol% SiO₂, 25 mol% Na₂CO₃, 9 mol% Al₂O₃, and 6 mol% CaO. The resultant cullet glass of the SiO₂-Na₂CO₃-Al₂O₃-CaO were dried and milled into powders. The Ce³⁺:YAG crystals were then uniformly mixed with the mother glass and sintered at 750°C for 1 hour and annealed at 350°C for 3 hours, followed by cooling to room temperature. The concentration of Ce³⁺:YAG with 40 wt% exhibited higher luminous efficiency and provided better purity for the yellow phosphor-converter layers [6-8].

3 Design and fabrication of high-beam laser headlight module (LHM) and low-beam LED headlight module (LEDHM)

Figure 1 shows an integrated smart laser headlight with Lidar, which includes of a high-beam laser headlight module (LHM), a low-beam LED headlight module (LEDHM), and a LiDAR module [1]. The high-beam LHM consisted of two blue laser diodes, two blue LEDs, a yellow glass phosphor-converter layer with a copper thermal dissipation substrate, and one parabolic reflector to reflect blue light and yellow phosphor light combined into white light output, as shown in Fig. 2. A reflow solder technique for mounting

the glass converter on the copper substrate was used.

Nichia blue lasers with wavelength of 445-nm were used. The LHM exhibited a total output optical power of 9.5 W, a luminous flux of 4000 lm, a relative color temperature of 4,300 K, and an efficiency of 420 lm/W. The infrared thermal imaging camera showed that the temperature profile of the LHM with copper substrate was an average temperature of 48°C after an operation time of more than one hour. A flat-refractor was used to integrate the two blue laser beams together and was reflected into the glass phosphor-converter layer. The parabolic reflector improved the white light pattern of the LHM to satisfy the ECE R112.

Figure 3 shows the ray tracing diagram and distribution pattern of the high-beam LHM using simulation software SPEOS. In this study, the eye safety is an important issue since high power lasers are used. A sensor, as indicated by a blue rectangle below the white light source, as shown in Figure. 2, will be installed to monitor the proper function of the glass phosphor layer. In case of failure, the blue lasers will be turned-off. The high-beam patterns of the LHMs were measured and simulated, as shown in Table 1[1]. The high-beam patterns of the LHM were measured to be 180,000 luminous intensity (cd) at 0°(center), 84,000 cd at $\pm 2.5^\circ$, and 29,600 cd at $\pm 5^\circ$, which were well satisfied the ECE R112 class B regulation. The range of high-beam headlight was measured more than 300 m.

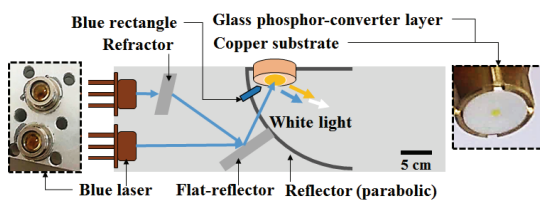


Figure 2 - Schematic diagram of high-beam LHM [1].

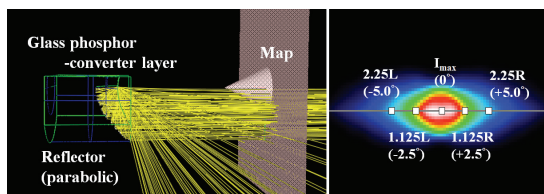


Figure 3 - Simulation of ray tracing diagram and 2D intensity distribution pattern for high-beam LHM [1].

Test point	Class B (cd)	Simulation (cd)	Measurement (cd)
I _{max} (0°)	> 40,500	189,777	180,000
H-1.125L/R ($\pm 2.5^\circ$)	> 20,300	88,740	84,000
H-2.25L/R ($\pm 5.0^\circ$)	> 5,100	35,726	29,600

Table 1. Measurement, simulation, and the specification of ECE R112 class B for high beam LHM [1].

Figure 4(a) shows a schematic diagram of low-beam LED headlight module (LEDHM). This LEDHM consisted of five blue LEDs, an elliptical-reflector, a mask, an

aspherical lens, and glass phosphor-converter layers on copper substrate, as shown in Fig. 4(b). OSRAM blue LEDs with wavelength of 445-nm were used. The LEDHM exhibited a luminous flux of 3100 lm, a correlated temperature of 6,000 K, and an efficiency of 310 lm/W. Figure 5 shows the simulation of ray tracing results and the 2D intensity distribution pattern of LED low-beam module. In the low-beam headlight, an asymmetric cut-off line was necessary to illuminate distance and significantly prevent the amounts of light from being cast into the eyes of drivers of the oncoming vehicles, as indicated in Figure. 5(b). The shape of cut-off line was horizontal on the left side and slanted at 15° to the right or angled at 45° degree to the horizontal, as shown in Figure. 5(b).

The low-beam patterns of the LEDHMs were measured and simulated, as shown in Table 2 in which all of the test points were well followed the low-beam of the ECE R112 [1]. The low-beam patterns of the LEDHM were measured to be 44,800 luminous intensity (cd) at Zone I, 448 cd at Zone III, and 3,158 cd at Zone IV, which were well satisfied the low-beam of the ECE R112 class B regulation. The difference between the measurement and simulation of the patterns could be caused by fabrication and assembly error.

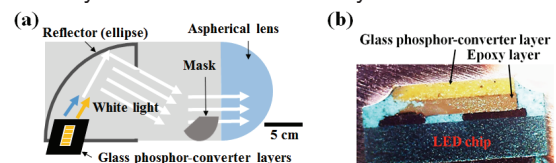


Figure 4 - (a) Schematic diagram of low-beam LEDM. (b) The cross section of glass phosphor-converter layers [1].

4 Package and measurement of LiDAR sensor

A LiDAR module embedded in smart laser headlight module (LHM) with the LiDAR detection software is shown in Fig. 6. With the feedback of the LiDAR, a smart LHM can control the headlight field, avoiding high-reflection areas at night and pay attention to all directions to ensure safe driving.

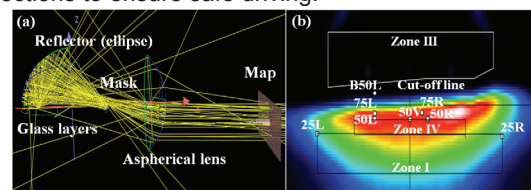


Figure 5 - Simulation of (a) ray tracing diagram and (b) 2D intensity distribution pattern for LED low-beam module [1]

The light source of LiDAR (low part of Fig. 6(a)) was a 905-nm laser emitter combined with diffractive optics that provided a wide illumination beam with viewing angle of 48° (horizontal) \times 3° (vertical). The telemeter of working on time-of-flight was 40-m, the signal was

generated by pulse with wavelength of 905-nm, and the optical power was 2W. The receiver assembly (up part of Fig. 6(a)) included 8 independent detection elements with simultaneous multi-object measurement capabilities supported by software with signal processing algorithms, as shown in Fig. 6(c).

Test point	Class B (cd)	Simulation (cd)	Measurement (cd)
B 5 0 L	≤ 350	105	330
7 5 R	≥ 10,100	12,800	12,880
7 5 L	≤ 10,600	9,950	7,840
5 0 L	≤ 132,00	11,160	7,280
5 0 R	≥ 10,100	10,890	28,000
5 0 V	≥ 5,100	10,710	11,088
2 5 L	≥ 1,700	4,337	17,360
2 5 R	≥ 1,700	4,383	15,120
Test point	Class B (cd)	Simulation (cd)	Measurement (cd)
Point 1+2+3	≥ 190	950	952
Point 4+5+6	≥ 375	1,350	1327
Point 7	≥ 65	423	470
Point 8	≥ 125	500	554
Zone III	Class B (cd)	Simulation (cd)	Measurement (cd)
	≤ 625	536	448
Zone IV	Class B (cd)	Simulation (cd)	Measurement (cd)
	≥ 2,500	8,528	3158
Zone I	Class B (cd)	Simulation (cd)	Measurement (cd)
	≤ 56,000	9,682	44,800

Table 2. Measurement, safety accreditation of ECE R112 class B, and simulation for low-beam LED module [1]

The detected multi-objects were shown in the green lines at 20-m. Using optical path and wavelength differences, the optical signal of LiDAR did not interfere with laser headlight. Therefore, high quality optical data could be obtained.

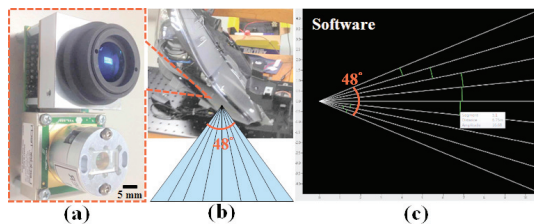


Figure 6 - (a) LeddarVu8-Medium, (b) embedded LiDAR module in smart laser headlight (c) software of signal processing algorithm [1]

5 Recognition of smart LHM

In this study, a simple method using the Hue Saturation Value (HSV) to determine detection and tracking robustness of the vehicle is proposed [1]. The HSV method can describe colors in terms of their shade and brightness. Employing HSV method, the recognition rate of vehicle and the brightness/shade area used to control the headlight are determined. This provides the driver with a better view and significantly improves road traffic safety.

We define a 6x2 region of interest (ROI) in the headlight-illuminated area according to the range of driver visibility reducing the computational complexity and the possibility of misjudgment. When the lights entered the ROI area, the position of the vehicles was marked with the blue squares and blue crosses in the image area through the recognition software, as shown in Figure 7(a). For the case 2 in Figure 7(b), we assumed that a

pedestrian and the lights entered the ROI area, the position of a pedestrian and lights were marked with a blue square (CCD image), a red square (LiDAR data), and distances (LiDAR data), which the ROI area was marked by the recognition software. According to the design of the smart laser headlight, when the vehicles and pedestrians enter the ROI areas, the smart laser headlight will be turned off at these areas. After the vehicles and pedestrians leave the ROI area, the smart laser headlight will be turned on again. To demonstrate the cases where the sensor misses the objects in the ROI areas or produces positive signal without any objects, the video sequences have been manually labelled. The video resolution was 960 x 540 when testing was conducted. The detection algorithm was evaluated by measuring bounding box intersection between annotation and the bounding box obtained by grouping detection. If the intersection percent was more than 70%, the detection was proclaimed as valid. The experimental results showed the correct detections of 702, missed detections of 97, and false positives of 31. Therefore, the detection rate was evaluated to be as 86%. The combination of the LiDAR sensor signals and CCD image signals resulted in a higher certainty in object detection compared to using the CDD image signals alone.

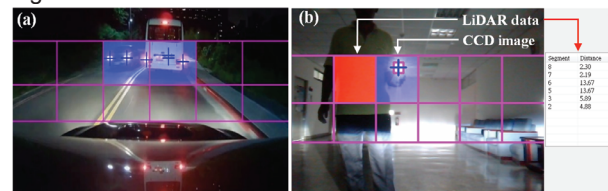


Figure 7 - Detection of ROI areas for (a) case 1 and (b) case 2 [1]

6 Smart Headlight and LiDAR using a single DMD

A novel system as shown in Figure 8 will be presented in which both function will use the same DMD. When the standard DMD operates, each mirror switches between 0° and -12°. This system uses the capability of the DMD in the ±12°. When the illumination light source is place at the -24° position as shown in the figure, the light will be reflected to the 0° position as output when the mirror is at the -12° position, which is the ON-position for the headlight. When the DMD is OFF with the mirror at the +12° position, the light is reflected to the 48° position, which is the OFF position, with light directed away from the output direction. The light is then absorbed by a heat sink to avoid the spilling of light into the detector.

Making use of the DMD's capability operating between -12° and +12°, the LiDAR laser beam is illuminated at the target and the reflected beam is collected at the 0°, which is reflected by the DMD either in the -12° or +12° positions. At the detection position of +12°, the reflected LiDAR signal will be directed to the

detector at the $+24^\circ$ position. When the DMD mirror is at the -12° , the reflected LiDAR signal will be directed to the -24° position where the light dump 2 and the headlight light source are. When the selected position of the DMD, corresponding to the location of the LiDAR beam, is set to have the mirrors switched to the $+12^\circ$ position, the reflected signal from the selected location will be directed to the detector for Z-direction determination as described previously. When the selected position of the DMD is “scanned” along the whole DMD area, such as raster scanning”, the full Z-positions of the target could be determined. This is the function of the scanning LiDAR where the scanning function is performed by the mirror switching of the DMD.

For the smart headlight function, the headlight source is position at the -24° position where the light will be reflected towards the output (0°) position towards the roadway when the mirror is at the -12° position. When the mirror is at the $+12^\circ$ position, the light will be reflected to the $+48^\circ$ direction and absorbed by the light dump 1. The net effect is that at the selected positions of the LiDAR detection, the headlight will be OFF at these positions and the light will be directed to the light dump 1 ($+48^\circ$). For all the un-selected position where the mirrors are at the -12° positions, the light will be output to the target as the headlight output beam. Since the selected area is synchronized to the scanning laser beam, the scanning laser beam does not illuminate these un-selected areas and these mirrors could also be switched to $+12^\circ$ without affecting the LiDAR detection function. As a result, this section of the mirrors can be used to switch off the headlight output as desired achieving the function of a smart headlight.

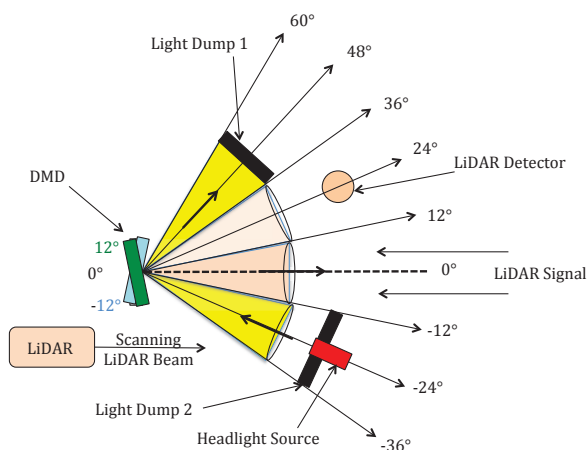


Figure 8 – Integrated Smart Headlight and LiDAR using a Single DMD

7 Conclusions

In summary, a new scheme of LiDAR embedded smart laser headlight module (LHM) for autonomous vehicles was proposed and demonstrated using a unique glass

phosphor-converter layer, which exhibited excellent thermal stability. The results were well satisfied the ECE R112 class B regulation. Employing a smart algorithm through the integration of the LiDAR sensor signals and CCD image signals, the generation of smart on/off signals for controlling the laser headlights was demonstrated. A patent pending design of a smart headlight integrated with a LiDAR sensor using a single DMD is also described.

8 Acknowledgement

This work was partially supported by the Ministry of Science and Technology under the contracts MOST 107-2218-E-005-025

REFERENCES

- [1] Y.P. Chang, C.N. Liu, Z.W. Pei, S.M. Lee, Y.K. Lai, P. Han, H.K. Shih, and W.H. Cheng, “New scheme of LiDAR-embedded smart laser headlight for autonomous vehicles,” *Opt. Express*, Accepted in 2019.
- [2] L.U. Lrich, “Whiter bright with lasers,” *IEEE Spectrum* 50(11), 36–56 (2013).
- [3] L. Wang, R.J. Xie, T. Suehiro, T. Takeda, and N. Hirotsaki, “Down-conversion nitride materials for solid State lighting: recent advances and perspectives,” *Chem. Rev.* 118(4), 1951–2009 (2018).
- [4] M. Cantore, N. Pfaff, R.M. Farrell, J.S. Speck, S. Nakamura, and S.P. DenBaars, “High luminous flux from single crystal phosphor-converted laser-based white lighting system,” *Opt. Express* 24(2), A215–A221 (2016).
- [5] K. Yoshimura, K. Annen, H. Fukunaga, M. Harada, M. Izumi, K. Takahashi, T. Uchikoshi, R.J. Xie, and N. Hirotsaki, “Optical properties of solid-state laser lighting devices using SiAl on phosphor-glass composite films as wavelength converters,” *Jpn. J. Appl. Physics* 55(4), 042102.1–042102.5 (2016).
- [6] J. Wang, C.C. Tsai, W.C. Cheng, M.H. Chen, C.H. Chung, and W.H. Cheng, “High thermal stability of phosphor-converted white light-emitting diodes employing Ce:YAG-doped glass,” *IEEE J. Sel. Top. Quantum Electron.* 17(3), 741–746 (2011).
- [7] Y.P. Chang, J.K. Chang, W.C. Cheng, Y.Y. Kuo, C.N. Liu, L.Y. Chen, and W.H. Cheng, “New scheme of a highly-reliable glass-based color wheel for next-generation laser light engine,” *Opt. Mater. Express* 4(1), 121–128 (2017).
- [8] Y.P. Chang, J.K. Chang, W.C. Cheng, Y.Y. Kuo, C.N. Liu, L.Y. Chen, and W.H. Cheng, “An advanced laser headlight module employing highly reliable glass phosphor,” *Opt. Express* 27(3), 7627–7628 (2019).
- [9] Leddar Vu8 Solid-State LiDAR, LeddarTech Inc., Quebec City, QC, Canada.